



# Mapping Multivalency and Differential Affinities within Large Intrinsically Disordered Protein Complexes with Segmental Motion Analysis\*\*

Sigrid Milles and Edward A. Lemke\*

**Abstract:** Intrinsically disordered proteins (IDPs) can bind to multiple interaction partners. Numerous binding regions in the IDP that act in concert through complex cooperative effects facilitate such interactions, but complicate studying IDP complexes. To address this challenge we developed a combined fluorescence correlation and time-resolved polarization spectroscopy approach to study the binding properties of the IDP nucleoporin153 (Nup153) to nuclear transport receptors (NTRs). The detection of segmental backbone mobility of Nup153 within the unperturbed complex provided a readout of local, region-specific binding properties that are usually masked in measurements of the whole IDP. The binding affinities of functionally and structurally diverse NTRs to distinct regions of Nup153 can differ by orders of magnitudes—a result with implications for the diversity of transport routes in nucleocytoplasmic transport.

How intrinsically disordered proteins (IDPs) can accommodate their exceptional binding diversity and function as hub proteins in the interactome is a largely unresolved question. Despite various advances in the past,<sup>[1]</sup> it remains a challenge to analyze IDP complexes, especially when the IDP maintains a high degree of disorder when bound.<sup>[2]</sup> In order to tackle this issue and analyze the various regions of the IDP that are involved in binding, it is common to use protein truncations. However, it has become abundantly clear that disruption or deletion of binding sites can neglect cooperative effects or long-range mechanisms, such as dynamic allosteric interactions.<sup>[3]</sup> Individual binding sites in IDPs are often as simple as short linear motifs<sup>[4]</sup> or single side-chain modifications, such as phosphorylation.<sup>[1b,5]</sup> Prominent examples include kinase substrates, such as the IDP Sic1 that maintains its disorder when bound to Cdc4.<sup>[1b]</sup> Only a single binding site of Cdc4 seems to be involved, making the interaction monovalent, even though the number of phosphorylations in the IDP can influence the binding strength.<sup>[3c,6]</sup> Large protein complexes can have tremendously

more intricate interaction dependencies,<sup>[3a,7]</sup> and studies that only probe the global behavior of a complex, such as the dissociation constant ( $K_d$ ), can give an incomplete view.<sup>[3b]</sup>

Here we demonstrate that time-resolved fluorescence anisotropy measurements paired with correlation spectroscopy and site-specific protein labeling can detect differential segmental backbone flexibility within IDPs when bound to their interaction partners. This technique can be exploited to identify local binding strengths between IDPs with multivalent interaction sites and interaction partners with one or multiple binding sites. The unexpectedly high dynamic range of the method makes it possible to assess sequence-specific binding affinities across several orders of magnitude within the same IDP, with no apparent size limit on the IDP to be analyzed.

We used this approach to study complexes of the large, phenylalanine-glycine (FG)-rich IDP nucleoporin153 (Nup153).<sup>[8]</sup> Such FG-repeat nucleoporins (FG-Nups) are central to the permeability barrier of the nuclear pore complex (NPC), which, as the largest molecular machinery in the cell, regulates the transport across the nuclear envelope.<sup>[9]</sup> A key feature of the transport mechanism is the interaction between these FG repeats and folded nuclear transport receptors (NTRs) that shuttle their cargo through the pore.<sup>[10]</sup> As NTRs typically have more than one FG binding site, and FG-Nups have multiple FG motifs (Nup153 has 24), their interactions are simultaneously “one to many” and “many to one” and thus constitute a highly multivalent binding problem (illustrated in Figure 1b).<sup>[9,11]</sup> The situation is even more complex, because the sequence of most FG-Nups, including the particularly large and multifunctional<sup>[12]</sup> Nup153, obeys a nonrandom but heterogeneous sequence composition and displays different types of FG repeats (as defined by neighbouring residues, Figure 1a). As FG-Nup sequence is not conserved across species, and due to the complexity of the NPC and the still elusive character of the permeability barrier, molecular understanding of how the FG-Nup sequence correlates with functionality and receptor binding is still limited.<sup>[13]</sup> Therefore, an improved understanding on region-specific functionality can majorly contribute to understanding a vital protein translocation pathway.

Protein binding and the number of proteins bound to each other can be approximated by analyzing the hydrodynamic properties of the protein or protein complex. Fluorescence correlation spectroscopy (FCS) and time-resolved fluorescence anisotropy both probe the hydrodynamic radius of a labeled protein by measuring translational and angular diffusion, respectively.<sup>[14]</sup> We site-specifically attached the

[\*] Dr. S. Milles, Dr. E. A. Lemke  
Structural and Computational Biology Unit, EMBL  
Meyerhofstrasse 1, 69117 Heidelberg (Germany)  
E-mail: lemke@embl.de

[\*\*] We are grateful to Dr. VanDelinder and Dr. Gibson, as well as the whole Lemke group, for helpful comments and discussions. S.M. acknowledges funding from the Boehringer Ingelheim fonds, and EAL from the Emmy Noether program of the DFG.

Supporting information for this article (including experiment details) is available on the WWW under <http://dx.doi.org/10.1002/anie.201403694>.

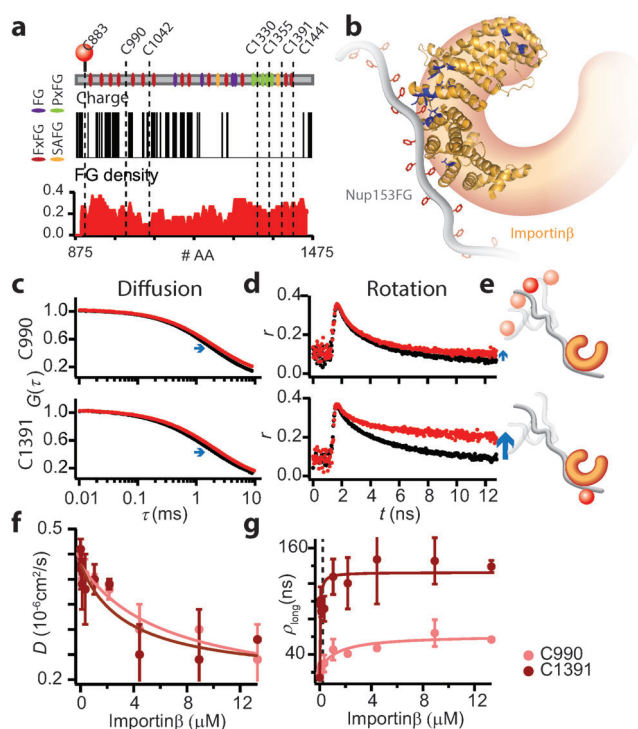


**Figure 1.** a) Scheme of Nup153FG with labeling sites indicated by dashed lines. b) Importinβ (PDB 1O6O) is orange with FG binding pockets in blue. Nup153FG is gray with Fs in red. c,d) Comparison of FCS ( $G(\tau)$  in (c)) and anisotropy ( $r$  in (d)) raw traces from labeled Nup153FG in the absence (black) and presence (red) of Importinβ with corresponding scheme of Nup153FG segmental motion (e) Importinβ titration with measured  $D$  (f) and  $r/\rho_{\text{long}}$  (g); dashed line at 1  $\mu\text{M}$  Importinβ.

fluorophore Atto655 near the N-terminus (C990, that is, 115 amino acids from the N-terminus) or near the C-terminus (C1391, that is, 80 amino acids from the C-terminus) of the Nup153 FG-rich domain (Nup153FG; amino acid numbering according to the full-length Nup153, Uniprot ID P49790), and measured diffusion and rotation. FCS curves were fit with a single diffusion coefficient ( $D$ ), and anisotropy decays were described by the two rotation times  $\rho_{\text{short}}$  (rotation of the dye around its linker) and  $\rho_{\text{long}}$  (protein rotation; see the Supporting Information (SI) and Figure S1 for more details). As the small fluorophore only minimally perturbs the protein, FCS ( $D$ , diffusion) and fluorescence anisotropy ( $r$ , rotation) measurements did not depend on the labeling position.

We next added an excess of the NTR Importinβ (97 kDa). Diffusion slowed down in agreement with complex formation similarly for both labeling mutants. However, in the rotational measurements, a large discrepancy was observed, with C990 ( $\rho_{\text{long}} \approx 30$  ns) rotating much faster than C1391 ( $\rho_{\text{long}} \approx 90$  ns; Figure 1 d). In line with a polymer physics view of IDPs, such an effect can be explained by segmental motion,<sup>[15]</sup> which predicts that individual segments in the polymer (polypeptide/protein) chain can rotate independently of other segments of the same protein. In agreement with previous studies on IDPs,<sup>[15]</sup> differential segmental motion was not detected in the unbound IDP. However, the result suggests that segmental motion can be used as readout to measure relative binding

strengths to regions near the labeling site in the large and dynamic complex. Our experiments thus indicate a stronger binding of Importinβ in the region of C1391 than in the region of C990.

If our rotational measurements are indeed characterized by segmental motion rather than rotation of the whole protein,  $\rho_{\text{long}}$  should not scale directly with the molecular weight (MW) of the protein if different-sized FG-Nups are analyzed. As shown in Figure 2 a, different-sized FG-Nup domains (yeast and human) indeed yielded a value of  $\rho_{\text{long}} = (12 \pm 1)$  ns averaged over all constructs that was thus independent of MW.  $D$  extracted from FCS measurements, however, scaled with MW linearly on a double-log plot.

To test the degree of sensitivity and robustness of segmental motion analysis for measuring region-specific binding properties in intact disorder-maintaining complexes, we first created partially binding deficient Nup153FG chimeras that had all F replaced by A in the PxFG or in the FxFG region, respectively (called Nup153FGAG and Nup153AGFG). FG→AG mutations disrupt the binding of Importinβ<sup>[17]</sup> and should therefore significantly affect segmental motion in the presence of Importinβ. We inserted labeling sites proximal to the N- and C-terminus (C883 or C1391) into these mutants, and measured diffusion and rotation in the presence and absence of Importinβ as described in Figure 1. While the diffusive properties of the chimeras were essentially unchanged compared to those of Nup153FG and the presence of Importinβ affected the diffusion of the different chimeras similarly, rotation was differentially influenced by the presence of the NTR. As Importinβ has markedly reduced affinity to AG regions, fluorescence anisotropy decays were influenced only when

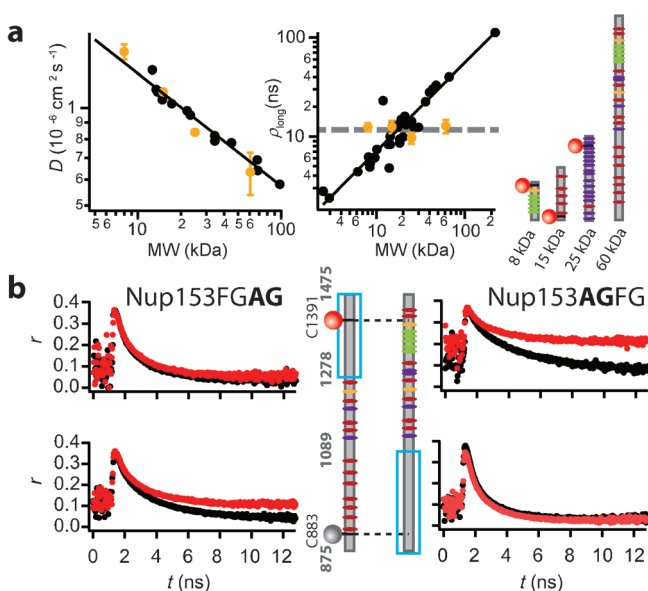


**Figure 2.** a) Diffusion and rotation of different-sized FG-peptides (scheme right, orange spheres with standard deviations in the graphs and dashed line as average). Black spheres are literature-known values of globular proteins with fit.<sup>[19]</sup> b) Raw data of labeled Nup153AGFG and Nup153FGAG in the absence (black) and presence of Importinβ (red) with corresponding schemes.

the fluorescence label was situated in an FG-containing region (Figure 2b, and Figure S2 for direct comparison with the wild-type). As shown in Figure S3, complementary FCS measurements with picosecond time resolution,<sup>[14,18]</sup> confirm the occurrence of segmental motion.

In the FCS measurements, both mutants had similar  $D$  values, so we can estimate a single apparent dissociation constant  $^D K_{d,app} \approx 1200$  nM from an Importin $\beta$  titration (Figure 1, and Figure S4, see SI Methods). Extracting an apparent dissociation constant  $^D K_{d,app}$  from the rotational analysis gives a very different picture with 1900 nM for C990 and 40 nM (i.e. 47-fold lower) for C1391. Even though at a concentration of 1  $\mu$ M Importin $\beta$ , the difference in  $\rho_{long}$  between C990 and C1391 is only threefold ( $\approx 30$  ns vs  $\approx 90$  ns), the titration captures site-specific  $^D K_{d,app}$  values that span several orders of magnitude within the same protein. It is also interesting to see that  $D$  becomes much smaller than expected from a 1:1 complex formation at high Importin $\beta$  concentrations, indicating that multiple (roughly seven) NTRs can bind to Nup153FG at the same time (Figure S5). Low  $^D K_{d,app}$  (even lower than  $^D K_{d,app}$ ) values can result from either region-specific stronger binding of one NTR, or from several NTR molecules simultaneously. Both scenarios can be interpreted as “stronger binding affinity” to the specific region and cannot easily be distinguished with the help of  $^D K_{d,app}$  measurements.

We then extended our study in a systematic fashion and performed  $D$  and  $\rho_{long}$  measurements for seven different Nup153FG mutants in the presence of Importin $\beta$ . Due to the sequence complexity and diversity of FG repeats in the middle region of Nup153FG, we limited the analysis to C-terminal and N-terminal regions in which FxFG and PxFG clusters are enriched, respectively (Figure 1a). In these experiments, we report values for  $D$  and  $\rho_{long}$  for a given, constant concentration of Importin $\beta$ , which delivers relative differences in NTR affinities, rather than  $K_{d,app}$  values for every one of the tested Nup153FG regions, for which a whole NTR titration would be necessary (see SI Methods). In agreement with the experiments in Figure 2, the seven different mutants reported a region-specifically resolved view of binding preferences, with  $\rho_{long}$  for C1391 sixfold enhanced compared to  $\rho_{long}$  for the weakest binding site of Importin $\beta$ , C1042 (Figure 3, Figure S6, and Table S1). As expected from the previous experiments,  $D$  did not substantially change between mutants ( $(0.50 \pm 0.06) \times 10^{-6} \text{ cm}^2 \text{ s}^{-1}$ ).

In the nucleocytoplasmic transport machinery, a variety of different NTRs exist that have different structures and functions.<sup>[10b]</sup> Motivated by the results with Importin $\beta$ , we next selected TRN1 (similar superhelical structure as Importin $\beta$ ) and NTF2 ( $\beta$ -sheet-rich dimer) to probe region-specific interactions with Nup153FG. We first optimized the protein concentrations such that  $\rho_{long}$  differed substantially from the unbound state and then performed diffusion and rotation measurements (see SI Methods for details). As upon interaction with Importin $\beta$ , the diffusion coefficient of Nup153FG is constant for the various labeling positions also when interacting with TRN1 and NTF2 ( $D_{TRN1} = (0.6 \pm 0.1) \times 10^{-6} \text{ cm}^2 \text{ s}^{-1}$  and  $D_{NTF2} = (0.63 \pm 0.15) \times 10^{-6} \text{ cm}^2 \text{ s}^{-1}$ ). Rotational measurements, however, revealed binding preferences

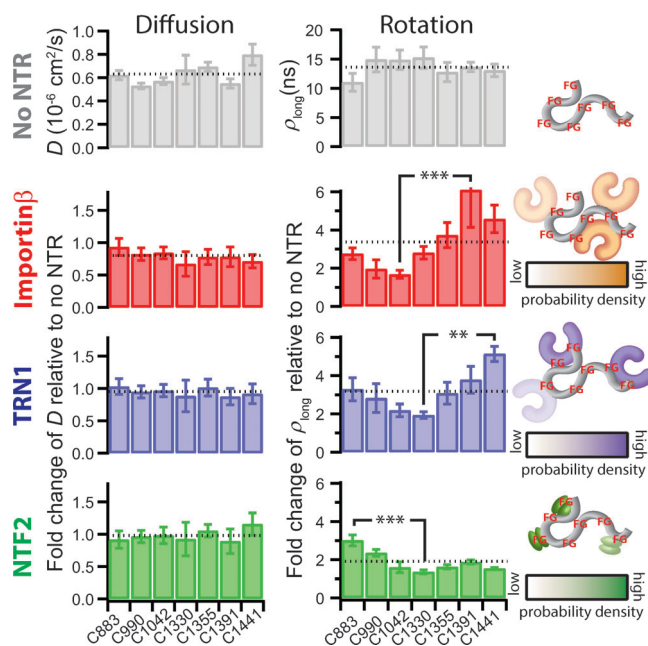


**Figure 3.** Comparison of  $D$  and  $\rho_{long}$  of Nup153FG alone. Fold changes are plotted in the presence of various NTRs (Importin $\beta$  = 1  $\mu$ M, TRN1 = 0.5  $\mu$ M, NTF2 = 10  $\mu$ M, see SI Methods for details). Dashed lines show averages over all mutants. For clarity, significance levels are shown only between the two most different values (\*\*  $p < 0.01$ ; \*\*\*  $p < 0.001$ ). Schematic representations of the differential binding probabilities are shown on the right.

of TRN1 and NTF2 on Nup153FG (Figure 3, Figure S6, and Table S1).

Affinities between FG-Nups and NTRs are a topic of long-standing discussion in the field, and due to the disordered nature of Nup153FG,  $K_d$  measurements are not easily established by classical biochemical techniques, such as analytical ultracentrifugation and gel shift assays. Furthermore, most previously used techniques can only measure affinities to entire FG-Nups (in vitro or in vivo) or truncations thereof (see for example, Ref. [19]). Our measurements provide a reproducible and robust readout of differential  $^D K_{d,app}$  values between different regions of Nup153FG and Importin $\beta$ . This highlights the multifaceted binding character even within a single FG-Nup. It is now tempting to speculate on the potential implications of our findings for nuclear transport. Independent of which transport model one considers,<sup>[8b,20]</sup> our differential binding properties of distinct NTRs to particular regions in Nup153 could be the molecular origin of different spatial routes.<sup>[10a]</sup> This would provide another level of regulation to the complex NPC mechanisms.

In summary, we have shown for an intricate and large IDP complex that segmental motion analysis can detect region-specific differences (fold changes in  $\rho_{long}$ ) in protein/ligand binding properties across several orders of magnitudes of apparent  $^D K_{d,app}$  values without perturbing the complex. While anisotropy measurements are standard in the fluorescence field to measure protein size, our anisotropy measurements did not scale with protein size (Figure 2), because IDPs can display high backbone flexibility.<sup>[15a]</sup> We detected no substantial differences in segmental mobility in the unbound Nup



for any of the mutants, despite the heterogeneous sequence composition of the IDP. Only upon formation of the Nup-Importin $\beta$  did we detect significantly different segmental motions. While our approach should be adaptable to any system that is flexible enough to display substantial segmental mobility, it is particularly relevant for disordered proteins within so-called “fuzzy” complexes.<sup>[2,7]</sup> Especially since low protein concentrations can be used compared to other techniques, our approach can also deal with aggregation-prone systems, such as Nup153FG.<sup>[21]</sup>

An upper detection limit is given by the requirement that  $\rho_{\text{long}}$  values have to be of similar magnitude as the fluorescence lifetime of the dye. Picosecond FCS measurements offer a higher dynamic range, but at the cost of more complex instrumentation and analysis.

Our approach therefore substantially extends the current repertoire of tools to minimally invasively study and locate functional sites without the need for generating truncation or deletion mutants. The variety of chemical biology tools that have been developed to install fluorescent labels even in intricate proteins<sup>[22]</sup> will facilitate the broad applicability of the method to the study of many large IDP complexes, which are highly abundant in the eukaryotic proteome.<sup>[3c,23]</sup> Our approach requires installation of only a single site-specific label, which is less demanding than intermolecular Förster resonance energy transfer (FRET) approaches. FRET would require labeling of the Nup and the Importin $\beta$ , a complex so large that it exceeds the dynamic range of FRET (3–10 nm).<sup>[14]</sup> Furthermore, as fluorescence is in principle a non-invasive technique, detection of segmental motion might even be used to study region-specific binding profiles within the cell in the future.

Received: March 25, 2014

Published online: June 4, 2014

**Keywords:** FG-nucleoporin · fluorescence · intrinsically disordered proteins · ligand binding · multivalency

- [1] a) K. Sugase, H. J. Dyson, P. E. Wright, *Nature* **2007**, *447*, 1021–1025; b) T. Mittag, S. Orlicky, W. Y. Choy, X. Tang, H. Lin, F. Sicheri, L. E. Kay, M. Tyers, J. D. Forman-Kay, *Proc. Natl. Acad. Sci. USA* **2008**, *105*, 17772–17777.
- [2] a) P. Tompa, M. Fuxreiter, *Trends Biochem. Sci.* **2008**, *33*, 2–8; b) M. M. Babu, R. W. Kriwacki, R. V. Pappu, *Science* **2012**, *337*, 1460–1461.
- [3] a) A. C. Ferreon, J. C. Ferreon, P. E. Wright, A. A. Deniz, *Nature* **2013**, *498*, 390–394; b) M. Fuxreiter, *Mol. Biosyst.* **2012**, *8*, 168–177; c) C. J. Oldfield, A. K. Dunker, *Annu. Rev. Biochem.*, DOI: 10.1146/annurev-biochem-072711-164947; d) J. H. Han, S. Batey, A. A. Nickson, S. A. Teichmann, J. Clarke, *Nat. Rev. Mol. Cell Biol.* **2007**, *8*, 319–330.
- [4] K. Van Roey, T. J. Gibson, N. E. Davey, *Curr. Opin. Struct. Biol.* **2012**, *22*, 378–385.
- [5] a) C. W. Lee, J. C. Ferreon, A. C. Ferreon, M. Arai, P. E. Wright, *Proc. Natl. Acad. Sci. USA* **2010**, *107*, 19290–19295; b) J. K. Lum, H. Neuweiler, A. R. Fersht, *J. Am. Chem. Soc.* **2012**, *134*, 1617–1622.
- [6] P. Nash, X. Tang, S. Orlicky, Q. Chen, F. B. Gertler, M. D. Mendenhall, F. Sicheri, T. Pawson, M. Tyers, *Nature* **2001**, *414*, 514–521.
- [7] M. Fuxreiter, P. Tompa, I. Simon, V. N. Uversky, J. C. Hansen, F. J. Asturias, *Nat. Chem. Biol.* **2008**, *4*, 728–737.
- [8] a) S. Milles, E. A. Lemke, *Biophys. J.* **2011**, *101*, 1710–1719; b) R. Y. Lim, B. Fahrenkrog, J. Koser, K. Schwarz-Herion, J. Deng, U. Aebi, *Science* **2007**, *318*, 640–643; c) A. A. Labokha, S. Gradmann, S. Frey, B. B. Hulsmann, H. Urlaub, M. Baldus, D. Gorlich, *EMBO J.* **2013**, *32*, 204–218.
- [9] S. Wälde, R. H. Kehlenbach, *Trends Cell Biol.* **2010**, *20*, 461–469.
- [10] a) J. Fiserova, S. A. Richards, S. R. Went, M. W. Goldberg, *J. Cell Sci.* **2010**, *123*, 2773–2780; b) A. Cook, F. Bono, M. Jinek, E. Conti, *Annu. Rev. Biochem.* **2007**, *76*, 647–671.
- [11] a) R. Bayliss, T. Littlewood, M. Stewart, *Cell* **2000**, *102*, 99–108; b) M. Rangl, A. Ebner, J. Yamada, C. Rankl, R. Tampe, H. J. Gruber, M. Rexach, P. Hinterdorfer, *Angew. Chem. Int. Ed.* **2013**, *52*, 10356–10359; *Angew. Chem.* **2013**, *125*, 10546–10549.
- [12] J. R. Ball, K. S. Ullman, *Chromosoma* **2005**, *114*, 319–330.
- [13] R. L. Adams, S. R. Went, *Cell* **2013**, *152*, 1218–1221.
- [14] E. Sisamakias, A. Valeri, S. Kalinin, P. J. Rothwell, C. A. M. Seidel, *Methods Enzymol.* **2010**, *474*, 455–514.
- [15] a) N. Jain, M. Bhattacharya, S. Mukhopadhyay, *Biophys. J.* **2011**, *101*, 1720–1729; b) A. Saxena, J. B. Udgaonkar, G. Krishnamoorthy, *Protein dynamics and protein folding dynamics revealed by time-resolved fluorescence*, Springer, New York, **2005**, pp. 163–179.
- [16] I. N. Serdyuk, *Methods in Molecular Biophysics: Structure, Dynamics, Function*, Cambridge University Press, Cambridge, **2007**.
- [17] S. S. Patel, M. F. Rexach, *Mol. Cell. Proteomics* **2008**, *7*, 121–131.
- [18] F. Hillger, D. Hanni, D. Nettels, S. Geister, M. Grandin, M. Textor, B. Schuler, *Angew. Chem. Int. Ed.* **2008**, *47*, 6184–6188; *Angew. Chem.* **2008**, *120*, 6279–6283.
- [19] a) J. Bednenko, G. Cingolani, L. Gerace, *J. Cell Biol.* **2003**, *162*, 391–401; b) I. Ben-Efraim, L. Gerace, *J. Cell Biol.* **2001**, *152*, 411–417; c) J. Tetenbaum-Novatt, L. E. Hough, R. Mironska, A. S. McKenney, M. P. Rout, *Mol. Cell. Proteomics* **2012**, *11*, 31–46; d) L. C. Tu, G. Fu, A. Zilman, S. M. Musser, *EMBO J.* **2013**, *32*, 3220–3230.
- [20] R. Peters, *Bioessays* **2009**, *31*, 466–477.
- [21] S. Milles, K. Huy Bui, C. Koehler, M. Eltsov, M. Beck, E. A. Lemke, *EMBO Rep.* **2013**, *14*, 178–183.
- [22] a) S. Milles, E. A. Lemke, *BioEssays* **2013**, *35*, 65–74; b) S. Milles, S. Tyagi, N. Banterle, C. Koehler, V. VanDelinder, T. Plass, A. P. Neal, E. A. Lemke, *J. Am. Chem. Soc.* **2012**, *134*, 5187–5195; c) I. Nikić, T. Plass, O. Schraidt, J. Szymanski, J. A. Briggs, C. Schultz, E. A. Lemke, *Angew. Chem. Int. Ed.* **2014**, *53*, 2245–2249; *Angew. Chem.* **2014**, *126*, 2278–2282.
- [23] P. Tompa, M. Fuxreiter, C. J. Oldfield, I. Simon, A. K. Dunker, V. N. Uversky, *BioEssays* **2009**, *31*, 328–335.